Open Research Online

Open Research Online

Predicting the particle-induced background for future X-ray astronomy missions: the importance of experimental validation for GEANT4 simulations

David Hall[*], Jonathan Keelan, Chris Davis, Oliver Hetherington, Mark Leese and Andrew Holland

Centre for Electronic Imaging, SPS, The Open University, Milton Keynes, MK7 6AA, UK

ABSTRACT

Particle-induced background, or "instrument background", produced from the interaction of background photons and charged particles with a detector, either as primaries or through the generation of secondary photons or particles, is one of the major sources of background for the focal plane sensors in X-ray astronomy missions. In previous studies for the European Space Agency (ESA) X-ray Multi Mirror (XMM-Newton) mission, the dominant source of background was found to be caused by the knock-on electrons generated as high-energy protons pass through the shielding materials surrounding the detector. From XMM-Newton, the contribution of Compton and other photon-generated background was small in comparison to the knock-on electron component. However, for the Wide Field Imager (WFI) on board the ESA Advanced Telescope for High-ENergy Astrophysics (ATHENA) mission Athena, which houses much thicker silicon in the depleted p-channel field effect transistor (DEPFET) active pixel sensors of the focal plane when compared to the Charge Coupled Devices (CCDs) used in the XMM-Newton EPIC MOS cameras, this photon component may no longer be expected to have such a minimal impact and therefore both the photon and proton-induced components must be considered in more detail.

In order to minimise the background, studies have been conducted on the use of a graded-Z shield in addition to an aluminium proton shield (employed for radiation damage minimization). For thin detectors, a low-Z component alone may suffice, reducing the fluorescence components of the background. However, with thicker detectors a high-Z component may give added benefit through the combination of the high-Z component to reduce the photon-induced effects and a low-Z component to reduce the fluorescence components from the shielding's inner-surfaces, thus creating an "aluminium sandwich". In all cases, careful optimization of the shielding configuration is required to balance each component of background specific to the design of the instrument involved. The optimization of any shielding relies heavily upon a validated and verified simulation toolkit. Here we present the latest progress on our ongoing validation and verification studies of the GEANT4 simulations used for such an optimization process through a series of experimental test campaigns.

Keywords: Radiation, instrument background, X-ray, DEPFET, CCD, GEANT4, Athena, WFI.

1. INTRODUCTION

The instrument background observed in-orbit for XMM-Newton was found to be significantly higher than that predicted before launch[1]. Detailed study of the background post-launch using simulations in the GEANT4 toolkit found that the soft-electron component, generated in the inner surfaces of the shielding and materials placed in the line of sight of the detectors, had been underestimated[2], bringing into light the complexity of the task of pre-launch simulations and prediction of instrument background. Whatever the ultimate cause of the background, one must aim to minimise the background to maximise the science possible with the mission. To this purpose, one technique that can be used to minimise the background is the use of graded-Z shielding. However, in order to optimise such shielding and to truly determine the likely impact of the shielding, simulations must be implemented; it would be near-impossible to subject a full spacecraft model to the full spectrum of incident particles experienced in-orbit through experimental testing. In order to have faith

in the results of the simulations one must first validate the simulations against experimental data, with particular attention required to the materials and particle energies that would dominate the spacecraft in orbit.The X-ray-like background of a silicon-based detector in space can be considered to be formed from two main components: the Cosmic X-ray Background (CXB) and the instrument background or 'quiescent non X-ray background'[3]. For the XMM-Newton EPIC cameras, the CXB was found to dominate below approximately 2 keV with the instrument background dominating at higher energies, giving a relatively simple form to the background itself, albeit the finer details of each of the two components being much more complex. Here we consider the instrument background to be the detection of any events in the detector that are indistinguishable from the X-ray events within the energy band of interest in the mission, be they generated from photons, electrons or other sources.

The direct detection of low energy CXB events is not the only source of background from the CXB however; for thicker detectors one can begin to see a non-negligible impact from Compton scattering of higher energy CXB photons. Although for the detector thicknesses of the XMM-Newton EPIC MOS of much less than 100 µm, the CXB component of the instrument background itself can be considered negligible in comparison to that of secondary low-energy electrons ejected from the shielding material[2], when much thicker detectors of several-hundred-microns are considered, the component of instrument background from the higher energy CXB photons becomes comparable to that of the low-energy electron production in the shielding. This balance must be considered carefully when making predictions on instrument background from the results of previous missions. As mentioned previously, the under-prediction of the level of instrument background for XMM-Newton was in part due to the assumption of the dominance of one component of background over another.

The Advanced Telescope for High ENergy Astrophysics (ATHENA) mission is an upcoming X-ray telescope that is designed to address the science theme of "The Hot and Energetic Universe". Due for launch in 2028, the mission will have a Halo orbit around the second Lagrange point (L2) and aims to answer two key astrophysical questions: how does ordinary matter assemble into the large-scale structures we see today and how do black holes grow and shape the universe?[4]. In combination with the telescope, two instruments will provide the capabilities to answer these questions: the X-ray Integral Field Unit (X-IFU) to provide spatiall-resolved high-resolution spectroscopy[5] and the Wide Field Imager (WFI)[6].

As Athena is likely to be placed into an L2 halo orbit, an understanding of the radiation environment at the second Lagrangian point (L2) is an essential ingredient in the determination of the instrument background for the mission. The second Lagrangian point is 1.5 million kilometres from the Earth, and so the radiation environment is similar to that of interplanetary space. The influence of particles trapped in the earth magnetic field is minimal, and the radiation belts are entirely avoided. What follows is a brief summary of the components of the radiation environment which are predicted to cause the majority of the instrument background within Athena's Wide Field Imager (WFI).

At L2 the most significant component of the radiation environment comes from solar and Galactic Cosmic Ray (GCR) protons. The quiescent solar proton component can be effectively shielded by a few centimetres of aluminium, however the majority of the GCR component is energetic enough that realistic levels of shielding fail to significantly attenuate the flux. The interaction of these high energy GCR protons are predicted to cause more than 50% of the total instrument background. There is an additional flaring component to the solar protons, however during periods of high intensity flares the instrument will not be performing observations, and so this component cannot contribute to the instrument background. The next most significant ionic flux comes from alpha particles, which occur at levels roughly an order of magnitude lower than that of the protons, with a similar spectral shape. Heavier ions are also present, but at fluxes which produce relatively little instrument background. A small flux of trapped electrons exists even at L2, and the interaction of these high energy electrons with the shielding can produce significant bremsstrahlung. Finally, there is the high energy (>30 keV) component of the CXB, which can fully penetrate the spacecraft shielding and interact directly with the detector.

The instrument background observed can vary greatly not only from mission-to-mission due to differing orbits (giving a differing incident particle spectra from which it is caused), but also between different detectors within the same spacecraft due to the camera system design[2,7,8], Figure 1. In most of the instrument background spectra shown, one can see clear fluorescence lines from the materials surrounding the detectors and often from the detectors themselves, shown most clearly in the aluminium and silicon fluorescence lines between 1-2 keV. At higher energies in some cases a much greater number of fluorescence lines can be seen, such as in the XMM-Newton EPIC-pnCCD; in this case the materials placed near the detectors, particularly the presence of a PCB directly behind the detector itself, cause additional fluorescence lines

to be observed and can lead to science loss within some energy bands if found to be too severely masked by fluorescence. The continuum from approximately 2-10 keV is thought to be dominated by two components: low energy electrons ejected from the inner surfaces of the surrounding shielding material and CXB-related Compton events (and those related to secondary photons generated by the GCR component). To a first approximation we can consider the low energy electron events to be from the inner most surfaces of surrounding materials because of the short absorption length of electrons of energy 2-10 keV such that any electrons generated deeper in the shielding would not be able to pass through the remaining shielding to reach the detector. For thinner detectors, such as the XMM-Newton EPIC-MOS and Swift-XRT (both using an e2v CCD22 with depletion region of 35-40 µm[9]), the electron component dominates, but for the thicker detectors such as the XMM-Newton EPIC-pnCCD (approximately 280 µm thick[10]), the increased thickness leads to a greater component of background from Compton scattering of CXB photons and therefore a higher background continuum. In addition, the surface structures of the device will have a major impact on the fraction of soft-electrons that reach the regions of the detector in which they will be detected. The final major feature seen in Figure 1 is the peak at around 10 keV and higher, such as shown in the Suzaku XIS1, caused by minimally ionised charged particles passing through the detector within an X-ray-like pixel pattern such that the energy deposited is proportional to the thickness of the detector. This component is of most concern for fully depleted, thinner detectors; if the detector is, for example, a CCD that is not fully depleted such as in the XMM-Newton EPIC-MOS case, then any charged particle tracks will spread over many pixels as the charge is collected in the pixels, and as the energy deposited is dependent on the thickness of silicon through which the particle travels, as the thickness of the detector increases the energy of the peak will also increase until the peak is outside of the energy band of interest.
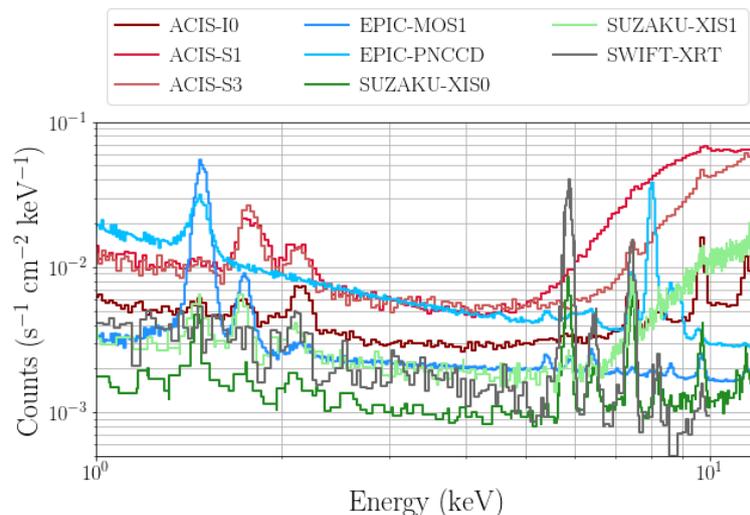

Figure 1. In-orbit instrument background spectra[11-14] shown for comparison between the EPIC MOS and pn-CCD cameras of the ESA XMM-Newton mission, the FI-CCD XIS1 and BI-CCD XIS0 of the JAXA Suzaku mission, the MOS CCD of the NASA Swift mission and the FI-CCD I0 and BI-CCDs S1 and S3 of the NASA Chandra ACIS. The different features of the spectra are a consequence of the mission orbit (defining the incident particle spectra) and the detector/camera design (defining the response to the incident particles).

The summary given above is, however, a somewhat simplified analysis of how instrument background is formed and the different components that form the background spectrum. In practice, many subtleties and fine balances come into play and it is often the case that reducing one component of the background results in an increase in a competing component. As an example, one can consider the simple case of adding more material into the shielding to reduce the flux of particles hitting the detector (e.g. to reduce the peak from minimally ionising charged particle tracks). This additional material will however lead to an increase in secondaries generated from GCR protons in the shielding, thus increasing a competing component of the background. It is therefore vital that all components of background are considered and that detailed studies are implemented in order to determine appropriate methods to reduce the overall background and presence of fluorescence peaks within the spectra.

2. MITIGATING INSTRUMENT BACKGROUND: GRADED-Z SHIELDING

A proton shield is designed to fulfil a primary aim of reducing the radiation damage in the detectors from high-energy protons. However, a large range of secondary particles are generated from proton interactions in such a shield and it is often these secondaries that dominate the incident background spectrum. In addition, for a detector of the 450 µm thickness of the DEPFETs to be used in the Athena WFI for example[15], there is a larger background component caused by CXB photons than would have been present within the thinner detectors of the XMM-Newton EPIC-MOS CCDs and pn-CCDs for example. In order to minimise the instrument background, additional layers of graded-Z shielding are required.

Graded-Z shielding is considered to be any shielding provided in addition to the proton shield of a different material (different atomic number, Z), primarily for the purposes of reducing instrument background. A graded-Z shield can be formed from a series of layers of material with atomic numbers above and below the aluminium of the proton shield, ultimately ending in an inner surface graded to low-Z materials to reduce X-ray fluorescence and/or move the energy of the fluorescence peaks outside of the energy window of main interest in the mission.

In its simplest form, one could consider a graded-Z shield to be created from an aluminium proton shield and an additional low-Z layer (e.g. beryllium) with sufficient thickness to absorb a large percentage of the aluminium fluorescence lines, and subsequently generating Be fluorescence with energy below 200 eV (i.e. out of the energy window of interest). Whilst this simple approach might be sufficient for a very thin detector in which the instrument background is purely dominated by a continuum of low energy electron events interspersed with fluorescence peaks, when the detector thickness increases, one must consider more carefully the incident CXB photons and also any secondary photon production.

In this more complex case, where the photon component is no longer negligible, a more developed graded-Z shielding approach is required, moving from high-Z outer layers through the aluminium proton shield to low-Z internal layers, thus creating an "aluminium sandwich" model. In addition, if a large quantity of secondary photons are produced within the bulk of the aluminium proton shield, an additional series of graded layers may be required, introducing a higher-Z material inside the aluminium shield before moving to lower-Z layers as before. A simplified diagram of such an approach is shown in Figure 2 (layer thicknesses not to scale). Optimising the layer combination is a complex process that is currently ongoing for the Athena WFI through the use of GEANT4 simulations (Section 3) alongside specific experimental campaigns (Sections 5-7).
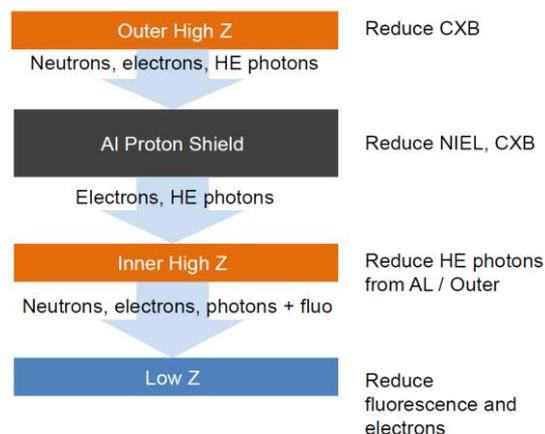

Figure 2. A schematic view of how graded-Z shielding may be approached to reduce instrument background, showing the main components of graded-Z shielding, with both high- and low-Z materials around a typical aluminium proton shield (an "aluminium sandwich" model). The main aims of each layer are shown on the right, although it should be noted that each layer will consequently reduce other components and may generate further secondaries. The final low-Z layer aims primarily to reduce the energy at which the final fluorescence photons that are emitted to be outside of the energy window of interest of the mission (or to reduce the fluorescence yield sufficiently through the use of a low-Z material), although the choice of material may have an impact on low energy electron generation.

3. SIMULATING INSTRUMENT BACKGROUND WITH GEANT4

In order to determine not only the level of instrument background expected in a mission, but also to design and provide the most suitable additional shielding to minimise the background, simulations can be carried out using the GEANT4 simulation toolkit[16]. Currently, such simulations are being carried out at the Open University as part of a wider simulation effort towards accurately predicting the instrument background that will be experienced by the Athena WFI and working towards a graded-Z shield configuration that will minimise the background as far as possible[17-20].

Several mass models of increasing complexity are often used to simulate the background, from a simple spherical shell model (minimising the run time required for the simulations) to a full CAD model of the instrument (maximising accuracy). Using the appropriate mass model, physics lists and input particle spectra, one can simulate images that may be observed in orbit, Figure 3. From these images background spectra can be produced and one can delve deeply into the production mechanisms for each background event recorded by following the background-producing particles back to their primary incident particle with any interactions along the way being tracked. Through use of results from the different mass models it is possible to gain both an understanding of the formation of the background and predictions of the background spectrum expected in orbit.

One cannot, however, blindly follow the results of the simulations with the assumption that the simulations are entirely valid. There are several issues regarding low energy processes within GEANT4, as discussed in Section 4. Indeed, studies are ongoing across a variety of different physics lists and processes as well as a focussed effort towards the production of validated physics lists for "space dedicated" projects and instrument background simulations[21]. However, for the Athena WFI, the results of these studies may be available only after the final shielding configurations have been designed, allowing verification of the designs but not facilitating use during the design process itself.

With these limitations in mind, we are implementing a series of experimental campaigns to test the materials and configurations proposed for the graded-Z shielding. As a consequence, the results can also be used to validate the simulations performed in GEANT4 in advance of the results for the AREMBES study being made available for use.
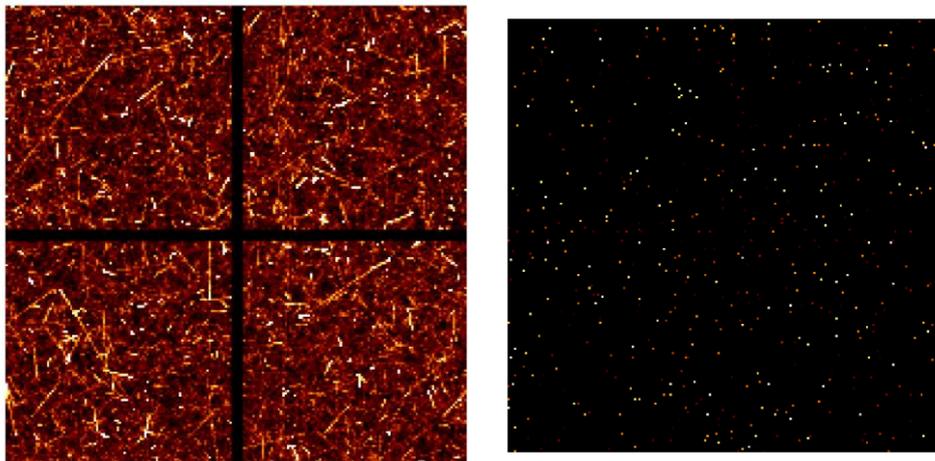

Figure 3. Left: A raw example image of all background events from a simple Athena WFI mass model, summed over several seconds. The proton tracks seen as lines across the image can be removed through processing. Right: After removing all events that do not appear as X-ray-like (from considering the pixels across which the signal is located in each event), only events that are indistinguishable from X-rays within the energy band of interest remain; it is these events that form the instrument background.

4. EXPERIMENTAL VALIDATION OF INSTRUMENT BACKGROUND SIMULATIONS

X-ray astronomy instrument background simulations require that GEANT4 maintain accuracy over a wide range of energies and a variety of physical processes. Comprehensive validation of fundamental physical processes such as bremsstrahlung production[22], electron energy deposition[23], electron backscattering[24] and PIXE[25] have been performed, and GEANT4 itself undergoes an extensive validation procedure after each update[26]. The majority of these validation efforts focus on energy ranges beyond those relevant to the background simulations of this paper, and as such the error introduced by GEANT4 to the background estimates is not well understood. Those validation efforts which span to relevant energy ranges show increasing disagreement with experiment, and that this disagreement worsened for materials with lower atomic numbers.

While investigating the basic physical processes involved in a GEANT4 instrument background simulation would provide a thorough understanding of its accuracy, it would do so only if all basic processes were validated. A simpler route is to perform validation against experimental data obtained from a fully representative experiment. For instrument background this implies the irradiation of shielding materials with high energy protons and measurement of the secondary radiation produced. Such a measurement, in addition to comparing the performance of various shielding solution, would provide a direct assessment of GEANT4 as an instrument background simulator.

While a comprehensive validation scheme would isolate each fundamental physical process and identify which processes cause the majority of the simulation error, such a scheme would be inherently complex and would require multiple experiments. The advantage of the outlined experiment is both its simplicity and potential to quickly evaluate the performance of shielding materials with respect to instrument background. To this end, an initial series of three experimental test campaigns is being undertaken, as outlined in Sections 5-7, the first of which has been already completed.

5. EXPERIMENTAL TEST CAMPAIGN 1: LOW ENERGY PROTONS (6 MEV)

In order to validate the performance of GEANT4 for instrument background simulations and shielding optimisation processes, we are carrying out a series of experimental test campaigns using proton energies and materials that are representative of those required for instrument background determination and shielding development. A series of three test campaigns form the first part of this study, with the first campaign completed at the Synergy Health proton facility at Harwell, UK.

For the first experimental test campaign, a series of foils were placed within the proton beam, under vacuum, at a 45 degree angle to the incident protons in a custom-designed vacuum chamber, Figure 4 (top left). At 90 degrees to the proton beam, a Teledyne e2v CCD97[27] was placed to record the secondary particles and photons generated in the foil whilst not being in the direct beam of primary protons. The CCD chosen for the testing was selected as it is capable of very low noise performance (sub-electron effective readout noise) at high readout speeds. Whilst the device performance and specifications are different to those of any particular mission in question, provided that the simulations use the correct detector, for the purposes of this validation the results will remain valid; we aim here to validate the simulations in terms of particle interactions in the foils and in the silicon of the detector.

Following the setup and installation of the test equipment for the first time, two foils were compared for the purposes of system testing and initial validation of the simulations: aluminium (100 µm thick) and copper (38 µm thick). As the observations are based primarily on what is emitted from the surface of the foil as the protons exit the samples, the thicknesses of the foils for the energies available at the facility (~6 MeV) were limited. Further testing of samples more comparable to the shielding that would be used in-orbit is scheduled in the third experimental test campaign at the Paul Scherrer Institute in Switzerland (Section 7).

The spectrum recorded for the aluminium foil sample is shown in Figure 5 (middle), with the events processed by the number of nearest-neighbour (nn) pixels that contain signal above the background. X-ray events would be expected to be single or double pixel events, as shown for the materials present (dominated by the aluminium foil, but also showing small peaks for materials present in the chamber and foil clamping system). The events that are spread across many pixels are currently assumed to be caused by low-energy electrons. The CCD97 used in the testing is a back-illuminated device and

therefore any low-energy electrons will interact at this back surface, leading to charge spreading across several pixels en route to the buried channel in the device. X-rays of the energies recorded here are more likely to interact further into the device, closer to the buried channel, and therefore spread over fewer pixels, as is observed.

An example GEANT4 simulated image is shown in Figure 5 (top), allowing the generation of a similar spectrum to that obtained experimentally for comparison. The raw GEANT4 simulated data (green) is shown to differ significantly from the experimental data (red). However, when one includes the aforementioned charge splitting through an additional charge diffusion model, the adjusted GEANT4 data (blue) is brought much closer to that of the experiment. However, it is seen in this early experiment that the results from the GEANT4 simulations (after being processed through the device simulation) still differ from the experimental results by up to 50%, significantly higher than the uncertainties on the proton flux (~10%) and count rates in the detector. This first test campaign was designed primarily to test the equipment and software and therefore further validation testing is required through the second and third test campaigns, along with a more detailed consideration of the charge spreading within the detector to determine the true extent of the disagreement between the simulated and experimental data.

Figure 4. Experimental equipment for tests performed during campaign 1 at the Synergy Health proton facility at Harwell, UK (~6 MeV).

6. EXPERIMENTAL TEST CAMPAIGN 2: VALIDATION BY PARTICLE TYPE

Following the initial test campaign on the Synergy Health proton facility at Harwell (UK), a second test campaign has been planned to allow a more in-depth assessment of the validity of the GEANT4 simulations. Alongside the additional experimental tests, a more detailed simulation of charge spreading within the device will be implemented on the GEANT4 simulated results to ensure a fair comparison of results is achieved.

In this second campaign, a magnetic field will be applied across the chamber, Figure 6. Through the use of a magnetic field of a few millitesla, the low energy electrons can be deflected away from the detector, allowing the separation of the photon and electron components of the background, Figure 7 and Figure 8. By separating the components, the two key causes of background in the experiment (low energy electrons and photons) can be independently validated and therefore the separate physics processes within the GEANT4 simulation tested.

The second experimental test campaign will again use protons of a much lower energy (~6 MeV) than those expected to dominate for the mission (~200 MeV). For this reason, a third campaign is planned to study the impact of more representative incident proton energies.
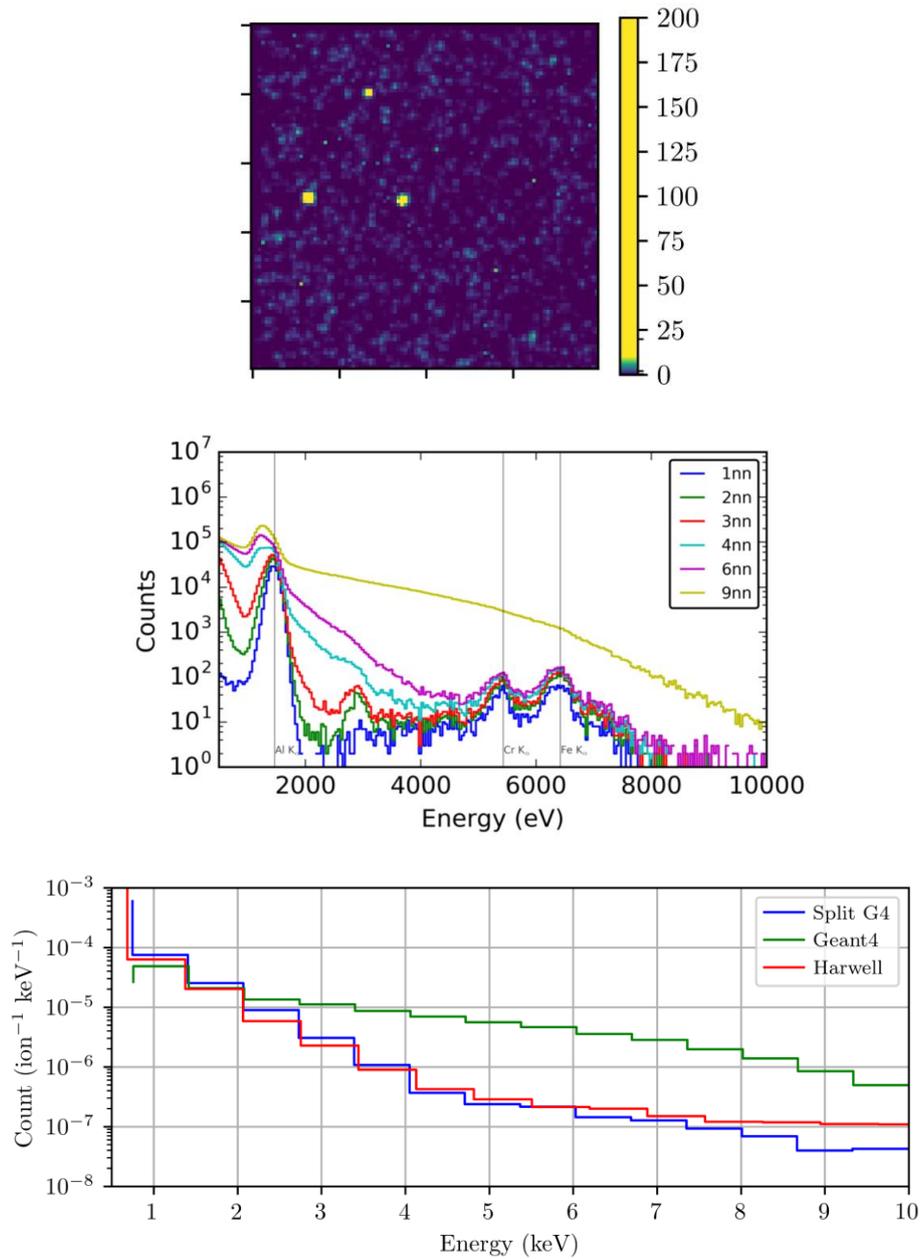
Figure 5. Experimental results from the first campaign, shown here for the aluminium sample. Top: Example simulated Geant4 simulated image showing the clear events that can be analysed and compared to the experimental images. Middle: Experimental data, split by event type in terms of the number of nearest neighbours (nn) above threshold. Bottom: The raw simulated data from GEANT4 (green) is seen to differ substantially from the experimental data (red), however, with additional processing of the GEANT4 data through the use of a bespoke device simulation to include charge spreading (blue), the GEANT4 data is seen to follow the same form as the experimental data, albeit differing by up to 50% in the energy range of interest. Further analysis is ongoing to determine the full extent to which the Geant4 simulations differ to the experimental results obtained.
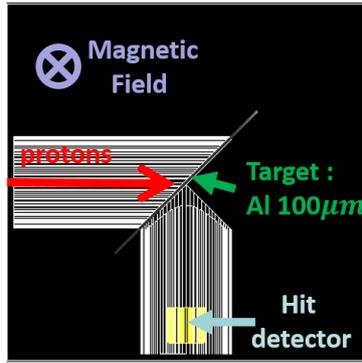
Figure 6. Schematic of the experimental equipment for tests to be performed during campaign 2 at the Synergy Health proton facility at Harwell, UK (~6 MeV) simulated in GEANT4 with the same geometry as that used in Figure 7.
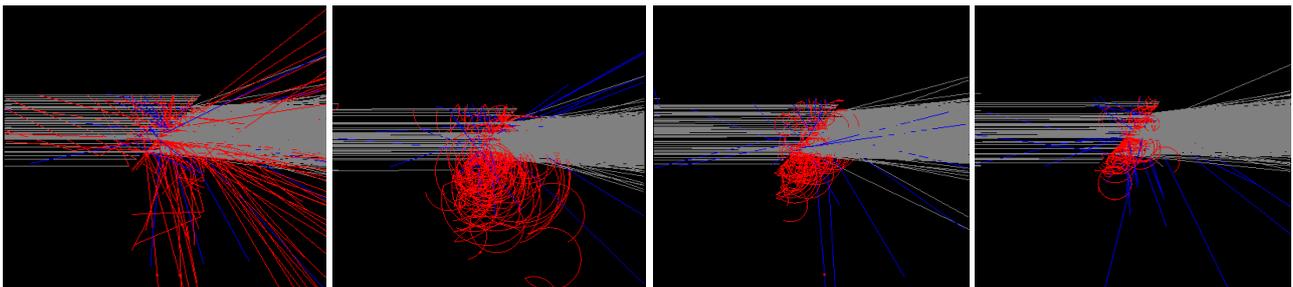

Figure 7. Using a magnetic field, the electron component of the background can effectively be switched off, allowing the electron and photon components to be separated. The experimental set-up is as per Figure 6, where here grey lines denote protons, red electrons, and blue photons. The magnetic field increases from left to right, shown for no field, 4 mT, 8 mT and 12 mT respectively, with the electrons (red) seen to no longer be able to reach the detector.
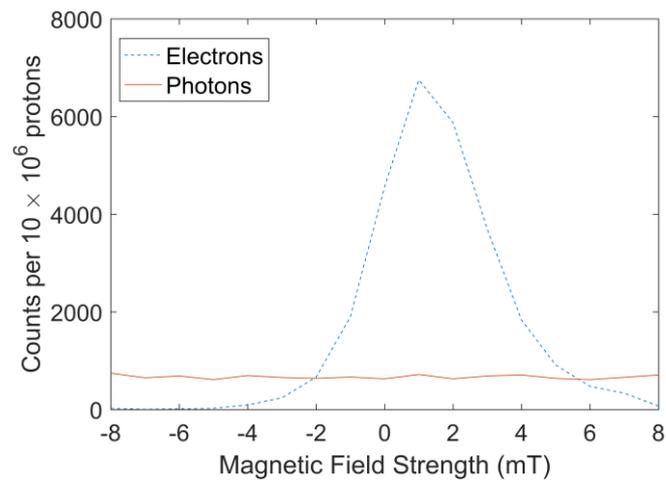

Figure 8. Through the application of a variation in the magnetic field strength, the electron component can be varied whilst the photon component remains constant, allowing the electron and photon components to independently validated. Simulated data is shown, demonstrating the expected change in counts that generate background events in the 0.1-15 keV energy range.

8. CONCLUSIONS

The minimisation of instrument background is vital to achieve the science goals of any space-borne X-ray astronomy mission. If not constrained through the use of appropriate shielding and camera design, the instrument background may obscure some (if not all) of the X-ray spectrum. Not only can the placement of different materials near to the focal plane lead to fluorescence lines within the spectrum, but the presence of all shielding materials must be considered with respect to the secondary particles and photons that are produced and may be detected within the focal plane camera.

In order to minimise the impact of fluorescence, a low-Z material inner layer may be added to absorb the fluorescence X-rays from previous layers and emit at a lower energy and with a lower fluorescence yield. To minimise the impact of secondaries generated within the bulk of the shielding (such as from the proton shield), additional high-Z materials may be required, both outside and possibly inside the proton shield. In this way, a true "graded-Z" shield, from high-Z materials through aluminium in the proton shield to low-Z materials, may evolve such that all components of the instrument background can be suitably minimised.

To optimise the design of such a shield, the GEANT4 simulation toolkit can be used. However, GEANT4 was primarily designed for use with higher energy particles and questions remain as to the validity at the energies of interest within instrument background studies. To this end, a series of experimental test campaigns have been planned with representative materials to allow validation against the simulations in representative conditions. At the time of writing, the first experimental test campaign, using ~6 MeV protons and thin foils, has been completed. A second campaign, again using thin foils, but with the addition of a magnetic field applied across the chamber, will enable a more detailed validation. A third campaign, moving to a higher energy proton beam (~200 MeV), will allow the testing of shielding candidates at full thicknesses (few centimetres) and, coupled with further developments in the device simulations applied to the GEANT4 outputs, will enable a true validation of the GEANT4 simulations in more representative conditions. Through this combined approach, using both GEANT4 simulations and experimental test campaigns, a truly optimised shielding configuration can be developed for future missions.

10. ACKNOWLEDGEMENTS

REFERENCES

[1] C. S. Dyer, P. R. Truscott, H. E. Evans, C. L. Peerless, IEEE, Transactions on Nuclear Science, 43 6 (1996).
[2] Hall, David J. and Holland, Andrew (2010). Space radiation environment effects on X-ray CCD background. Nuclear Instruments and Methods in Physics Research Section A: Accelerators, Spectrometers, Detectors and Associated Equipment, 612(2) pp. 320–327.
[3] De Luca, S. Molendi, Proc. Symposium 'New Visions of the Xray Universe in the XMM-Newton and Chandra Era' (2001)
[4] Athena mission proposal and white paper, K. Nandra, X. Barcons, D. Barret, A. Fabian, J.W. den Herder, L. Piro, M. Watson et al.
[5] Barret, D., den Herder, J. W., Piro, L., et al. 2013, An Athena+ supporting paper: The X-ray Integral Field Unit (X-IFU) for Athena, 2013, arXiv1308.6784
[6] Rau, A., Meidinger, N., Nandra, K., et al. 2013, An Athena+ supporting paper: The Wide Field Imager (WFI) for Athena, 2013, arXiv1308.6785
[7] Hall, D. J.; Holland, A. and Turner, M. (2007). Modelling instrument background for CCD x-ray spectrometers in space. In: SPIE Optics+Photonics 2007: Astronomical Optics and Instrumentation, 26-30 Aug 2007, San Diego, California, USA.

[8] Hall, David; Holland, Andrew and Turner, Martin (2008). Simulating and reproducing instrument background for x-ray CCD spectrometers in space. In: Proceedings of SPIE: High Energy, Optical, and Infrared Detectors for Astronomy III, 23-27 Jun 2008, Marseille.

[9] M. J. L. Turner, et al., A&A 365 (2001) L27-L35.

[10] L. Struder, U. Briel, K. Dennerl, et al., A&A 365 (2001) L18-L26.

[11] Carter, J. A.; Read, A. M., The XMM-Newton EPIC background and the production of background blank sky event files, Astronomy and Astrophysics, Volume 464, Issue 3, March IV 2007, pp.1155-1166.

[12] https://heasarc.gsfc.nasa.gov/docs/suzaku/prop_tools/xis_cxb.html (accessed 9th May 2018).

[13] C. Pagani, D. C. Morris, J. Racusin, D. Grupe, L. Vetere, M. Stroh, A. Falcone, J. A. Kennea, D. N. Burrows, J. A. Nousek, A. F. Abbey, L. Angelini, A. P. Beardmore, S. Campana, M. Capalbi, G. Chincarini, O. Citterio, G. Cusumano, P. Giommi, O. Godet, J. E. Hill, V. La Parola, V. Mangano, T. Mineo, A. Moretti, J. P. Osborne, K. L. Page, M. Perri, P. Romano, G. Tagliaferri, F. Tamburelli, "Characterization and evolution of the swift x-ray telescope instrumental background," Proc. SPIE 6686, UV, X-Ray, and Gamma-Ray Space Instrumentation for Astronomy XV, 668609 (13 September 2007).

[14] http://cxc.harvard.edu/ciao/download/caldb.html (accessed 9th May 2018).

[15] Norbert Meidinger, Josef Eder, Tanja Eraerds, Kirpal Nandra, Daniel Pietschner, Markus Plattner, Arne Rau and Rafael Strecker, The Wide Field Imager Instrument for Athena, SPIE 9905, Space Telescopes and Instrumentation 2016: Ultraviolet to Gamma Ray, 99052A (18 July 2016).

[16] S. Agostinelli et al., GEANT4 - A Simulation Toolkit, Nuclear Instruments and Methods A 506 (2003) 250-303.

[17] Fioretti, Valentina; Mineo, Teresa; Bulgarelli, Andrea; Dondero, Paolo; Ivanchenko, Vladimir; Lei, Fan; Lotti, Simone; Macculi, Claudio; Mantero, Alfonso, Geant4 simulations of soft proton scattering in X-ray optics. A tentative validation using laboratory measurements, Experimental Astronomy, Volume 44, Issue 3, 2017, pp.413-435.

[18] Molendi, Silvano, The role of the background in past and future X-ray missions, Experimental Astronomy, Volume 44, Issue 3, 2017, pp.263-271.

[19] Perinati, Emanuele; Barbera, Marco; Diebold, Sebastian; Guzman, Alejandro; Santangelo, Andrea; Tenzer, Chris, Preliminary assessment of the ATHENA/WFI non-X-ray background, Experimental Astronomy, Volume 44, Issue 3, 2017, pp.387-399.

[20] Kienlin, Andreas et al, Evaluation of the ATHENA/WFI instrumental background, SPIE Astronomical Telescopes and Instrumentation, 2018, in press.

[21] P. Dondero, A. Mantero, A ''Space dedicated'' GEANT4 physics list from the AREMBES project, SWHARD SRL, On behalf of the AREMBES WP3 and WP4 teams, 12th Geant4 Space User Workshop, 10-12 April 2017, University of Surrey, UK

[22] L. Pandola, C. Andenna, B. Caccia, Validation of the Geant4 simulation of bremsstrahlung from thick targets below 3MeV, Nuclear Instruments and Methods in Physics Research Section B: Beam Interactions with Materials and Atoms, Volume 350, 2015, Pages 41-48.

[23] M. Batič, G. Hoff, M. G. Pia, P. Saracco and G. Weidenspointner, "Validation of Geant4 Simulation of Electron Energy Deposition," in IEEE Transactions on Nuclear Science, vol. 60, no. 4, pp. 2934-2957, Aug. 2013.

[24] Basaglia, Tullio, et al. "Investigation of Geant4 simulation of electron backscattering." IEEE Transactions on Nuclear Science 62.4 (2015): 1805-1812.

[25] Mantero, A. , Ben Abdelouahed, H. , Champion, C. , El Bitar, Z. , Francis, Z. , Guèye, P. , Incerti, S. , Ivanchenko, V. and Maire, M. (2011), PIXE simulation in Geant4. X-Ray Spectrom., 40: 135-140.

[26] K. Amako et al., "Comparison of Geant4 Electromagnetic Physics Models Against the NIST Reference Data," in IEEE Transactions on Nuclear Science, vol. 52, no. 4, pp. 910-918, Aug. 2005.

[27] CCD97 Back Illuminated Datasheet, e2v technologies public document, A1A-CCD97BI_2P_IMO Issue 3, May 2004.